Mon. Not. R. astr. Soc. (1979) **187**, 553–566

Speckle interferometry in the near-infrared

M. J. Selby and R. Wade *Astronomy Group, Physics Department, Imperial College, London SW7*

C. Sanchez Magro *Instituto de Astrofisica de Canarias, Universidad de La Laguna, Tenerife, Canary Islands*

Received 1978 October 20; in original form 1978 June 20

Summary. A new technique to perform speckle interferometric measurements at J, H, K, L and M wavelengths is described. The time-averaged spatial frequency power spectrum of an image is obtained by scanning it successively over a series of gratings of differing spacing. Some measurements on a 1.5-m telescope are reported which show that diffraction-limited information is available at the near-infrared wavelengths. The point spread transfer functions of the speckle technique are predictably similar to ones measured at visible wavelengths. The size of the seeing disc at infrared wavelengths is measured and found to obey a $\lambda^{-1/5}$ law. Limiting speckle magnitudes for diffraction-limited resolution are generally derived and found to be approximately independent of telescope diameter. With long integration at $\lambda = 2.2\,\mu$m it should be possible to measure diffraction-limited information from sources with $m_K \simeq +12$ mag.

Introduction

Stellar speckle interferometry was originally suggested by Labeyrie [1] as a method for obtaining diffraction-limited information in the presence of a turbulent atmosphere. The technique was first implemented by Gezari, Labeyrie & Stanchnik [2] and is now well established at visible wavelengths with several groups obtaining useful results [3–7]. In this paper we discuss the feasibility of extending speckle interferometry to near-infrared wavelengths (1–5 μm) and present some initial measurements using a method which is necessarily different from that commonly used at visible wavelengths.

Generally the technique at visible wavelengths involves recording a large number of short exposure images of a star through a narrow bandwidth filter. The instantaneous image intensity may be expressed as:

$$I(\zeta, \eta) = O(\zeta, \eta) \otimes t(\zeta, \eta) \qquad (1)$$

where $O(\zeta, \eta)$ is the object intensity, $t(\zeta, \eta)$ is the instantaneous point spread function of the atmosphere/telescope system and $\otimes$ represents convolution.

Each of the short exposure images contains high spatial frequency information about the object, the cut-off frequency being equal to the diffraction limit of the telescope pupil [8, 9, 10]. If these images were simply co-added a characteristic seeing disc of about 1–2 arcsec would be obtained and the high spatial frequency information would be lost. Alternatively if their spatial frequency power spectra are co-added then diffraction-limited information is retrieved for many telescopes and seeing conditions prevailing in the visible. It is not possible uniquely to reconstruct an arbitrary object intensity function since the power spectrum contains no phase information, although methods have been suggested [11, 12] for its retrieval. It is useful, however, to obtain the equivalent angular widths, in the infrared, of assumed centro-symmetric objects such as binary systems and stellar shell structures.

In the spatial frequency domain the average power spectrum of the image intensity is given by

$$\langle |i(u,v)|^2 \rangle = |\mathrm{O}(u,v)|^2 \cdot \langle |T(u,v)|^2 \rangle \tag{2}$$

where $i(u,v)$, $\mathrm{O}(u,v)$ and $T(u,v)$ are the Fourier transforms of $I(\zeta,\eta)$, $\mathrm{O}(\zeta,\eta)$ and $t(\zeta,\eta)$ respectively. $\langle |T(u,v)|^2 \rangle$ is the transfer function of the speckle technique which Korff, Dryden & Miller [8] have shown to be insensitive to aberrations provided the optical system is of sufficient quality to resolve the atmospherically induced seeing disc, in which case:

$$\langle |T(u,v)^2| \rangle = |\langle T(u,v) \rangle|^2 + kT_{\mathrm{D}}(u,v) \tag{3}$$

where $\langle T(u,v) \rangle$ is the normal time-averaged transfer function associated with the seeing disc, $T_{\mathrm{D}}(u,v)$ is the diffraction-limited transfer function of the telescope aperture and k is a constant which depends on wavelength and seeing parameters. Although no detailed studies of infrared seeing have been reported, Young [13] suggests that the size of the seeing disc should be proportional to $\lambda^{-1/5}$ so that at $\lambda = 2.2\,\mu$m it is reduced by a factor of 0.74 compared to $\lambda = 0.5\,\mu$m. It is possible that in very good seeing conditions telescope aberrations will limit the available resolution, particularly at the longer wavelengths.

Infrared speckle method

Unfortunately the methods used in visible speckle interferometry are not suitable for use at infrared wavelengths since sensitive image-forming detectors are not available for wavelengths longer than about 1 μm. Arrays of detector elements are available but would be prohibitively expensive for this application and in our instrument a single element is used to

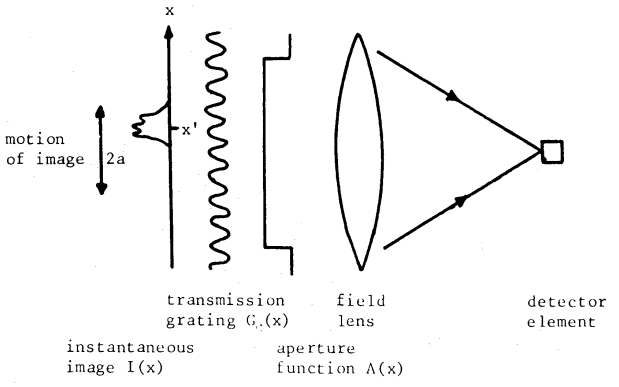

Figure 1. One-dimensional spatial frequency filter. $I(x)$, $G_\sigma(x)$ and $A(x)$ all lie in the focal plane of the telescope.

provide speckle measurements in *one dimension.* It is possible, however, to obtain information in orthogonal directions at differing times.

The time-averaged spatial frequency power spectrum of the instantaneous image $I(x)$ (in one dimension) is sampled sequentially using a series of spatial frequency filters which consist of transmission gratings in the focal plane of the telescope (see Fig. 1). With any one filter in position the image is oscillated across the grating normal to the grating lines using a triangle motion so that the signal received by the detector is modulated at a quasi-constant frequency. A modulation frequency of 120 Hz is used which is convenient for the detector system and at this rate the image remains 'frozen' during its motion over several periods of the grating. The image motion is programmed with constant amplitude and differing frequencies so as to maintain a constant modulation frequency over the entire range of gratings used. With a given chop amplitude the aperture size is carefully chosen so that the energy in the image remains well within the aperture.

With reference to Fig. 1, the image $I(x)$ is at an arbitrary position x' and the detector signal may be expressed as:

$$S_{\sigma'}(x') = I(x) \otimes [G_{\sigma'}(x) \cdot A(x)] \tag{4}$$

where $\sigma' = 2\pi/\lambda'$, and $1/\lambda'$ is the grating constant, $A(x)$ is the aperture function of width $2b$.

The transfer function of the spatial frequency filter is given by:

$$T_{\sigma'}(\sigma) = g_{\sigma'}(\sigma) \otimes a(\sigma) \tag{5}$$

where $g_{\sigma'}(\sigma)$ and $a(\sigma)$ are the Fourier transforms of $G_{\sigma'}(x)$ and $A(x)$ respectively.

Assuming $G_{\sigma'}(x) = \cos[\sigma' x + \phi]$, i.e. taking the fundamental only, with ϕ as an arbitrary phase factor, the filter $T_{\sigma'}(\sigma)$ is peaked at $\sigma = \pm\sigma'$ and has an 'equivalent' bandwidth $\Delta\sigma \simeq \pi/b$. If $b \gg \lambda'$, then $\Delta\sigma/\sigma' \ll 1$ and to a good approximation equation (4) may be re-written as:

$$S_{\sigma'}(x') = i_a(\sigma')\,\Delta\sigma \cos[\sigma' x' + \phi + \Phi(\sigma')] \tag{6}$$

where $i(\sigma) = i_a(\sigma) \exp[j\Phi(\sigma)]$ is the Fourier transform of $I(x)$.

Assuming for the moment that $I(x)$ is constant in time, it is evident that the mean power of the signal $S_{\sigma'}(x')$ is proportional to the spatial frequency power per unit bandwidth $i_a^2(\sigma)$ at $\sigma = \sigma'$ when averaged over an infinite range of x'. However, using an image motion of finite amplitude, a measure of $\langle |S_\sigma(x')|^2 \rangle$ leads to a systematic error in the assessment of $i_a^2(\sigma)$ which depends on the chop amplitude (a) and the phase factors ϕ and $\Phi(\sigma)$. The errors and the form of the signal $S_\sigma(x')$ are discussed in the Appendix in which we show that the use of coarser gratings must be restricted for finite chop amplitudes. These considerations are very relevant to the use of this method in the infrared since it is important to aim for small chop amplitudes so that the smallest aperture $A(x)$ can be used to reduce the large infrared background radiation received by the detector.

Instrument

A single element 0.5 mm^2 indium antimonide detector is cooled to 63 K, by pumping on liquid nitrogen; the arrangement inside the cryostat is shown in Fig. 2. The optical filters and transmission gratings are similarly cooled to reduce the sky/telescope infrared background. The relevant details of the optical filters covering the atmospheric windows are given in Table 1. The transmission gratings are barium fluoride discs coated with aluminium lines; the finest one used as 25 line/mm. A total of 12 gratings are mounted in a wheel placed at the focal plane of the telescope and a field lens focuses the telescope primary mirror on to the detector element.

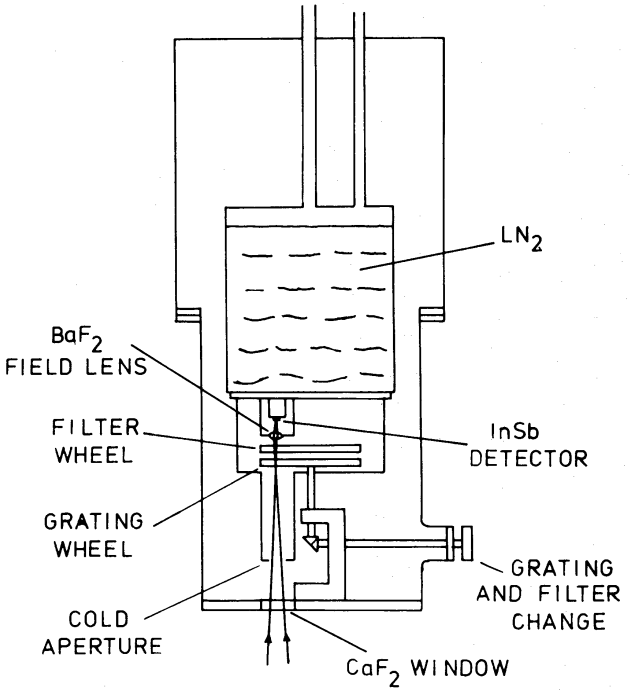

Figure 2. Detector cryostat.

Table 1. Details of infrared filters used. The dispersion is for zenith distance = 60° while the resolution $\Delta\theta_D = \lambda/D$ where D = 1.5 m.

	J	*H*	*K*	*L*	*M*
λ_{eff} (μm)	1.23	1.65	2.23	3.45	4.94
$\Delta\lambda_{phot}$ (μm)	0.24	0.30	0.41	0.57	0.80
$\Delta\lambda = \lambda^2/D\ \Delta\theta_s$ (μm)	0.12	0.24	0.46	1.20	2.65
Dispersion (arcsec)	0.123	0.062	0.033	0.021	0.0034
Resolution (arcsec)	0.17	0.23	0.31	0.47	0.68

The image is moved across a stationary grating rather than the reverse case, in order to avoid modulation of the background radiation. A two-mirror focal-plane chopper of a similar type to that described by Jorden *et al.* [14] is used to control the image motion. The two mirrors are mounted on cross-spring hinges, the angle between them being maintained at 90° by a parallelogram arrangement (see Fig. 3). The motion is imparted to the mirrors using

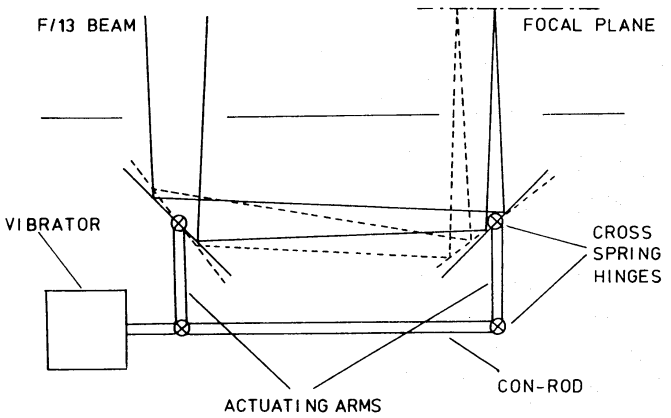

Figure 3. Two-mirror chopping system.

a Ling Dynamics System 200 vibrator and is servo-controlled using a magneto-resistive transducer mounted on one of the con-rods. Jorden *et al.* [14] and Koorneef [15] point out that it is possible by changing the actuator assembly slightly to ensure that the beam from the detector always 'sees' the same part of the primary telescope mirror, thus eliminating a possible source of background chopping signal. This modification is incorporated into the chopper by making one pair of actuating arms slightly longer than the other pair. However, the main advantage of the two-mirror chopper compared with the single mirror type for this application is that it produces a negligible amount of defocusing of the image. In practice good triangular image motions were obtained at the maximum programmed frequency (~30 Hz with chop amplitude of 1 mm) with negligible rounding-off at the peaks. It was found that satisfactory profiles could be obtained at frequencies in excess of 100 Hz with chop amplitudes up to 5 mm.

Data reduction method

A considerable amount of effort was made to reduce the computing time required to evaluate the power spectra of the speckle signals, which now has evolved so that it takes approximately one and a half times the observation time. The detector signals using any one transmission grating are recorded in analogue form on magnetic tapes which are later analysed using an Interdata 70 computer with CAMAC interfacing and two 2½ mega-byte magnetic discs. On-line analysis at the telescope has not been possible due to the high data rates required, although a computer-controlled spectrum analyser provides a 'quick look' facility during the observations. The spectrum analyser scans sequentially through the spectrum which results in a considerable loss of signal/noise ratio. Nevertheless on-the-spot assessments are particularly important with this technique as the most efficient mode of operation could be substantially different on differing nights.

All the data reduction computer programs are written in the high-level interactive language FORTH. This has enabled the rapid transfer of data to and from magnetic disc. After digitization at a rate of 400 sample/s, the data are stored in 512 number blocks on magnetic disc. The autocorrelation function is calculated for each block, co-added and then Fourier transformed to give the power spectrum. Using this method it is only necessary to perform a cosine Fourier transform on about 40 numbers to give a resolution in the power spectrum of ~5 Hz. Fig. 4 shows two examples of power spectra obtained using a bright

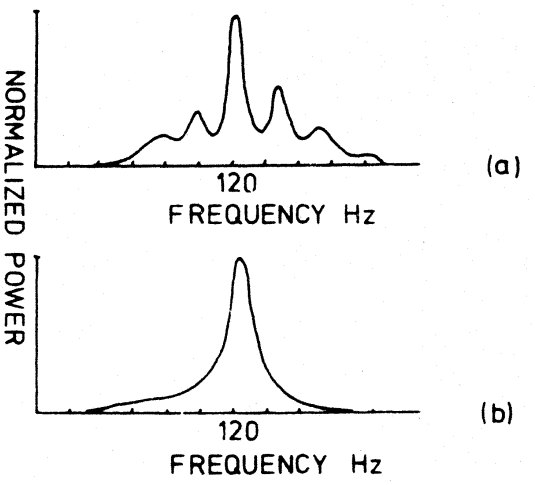

Figure 4. Power spectrum of signal from detector for: (a) grating with 2 line/mm, (b) grating with 7 line/mm. The star was μ UMa, observed at 2.2 μm.

calibration star. The integrated power spectrum over the modulation passband is used as a measure of the power in the image at the appropriate spatial frequency.

Observations

Infrared speckle measurements were taken during 1977 August and 1978 January at the Cassegrain focus of the 1.5-m telescope on Tenerife, Canary Islands. A set of infrared filters normally used for standard photometry through the J, H, K, L and M atmospheric windows was used. Korff [16] suggests that in order to avoid a loss in the visibility of the speckles, the bandwidth of the optical filters, $\Delta\lambda$, should be limited by the relation:

$$\Delta\lambda \simeq \lambda^2/D\,\Delta\theta_s \tag{7}$$

where $\Delta\theta_s$ is the diameter of the seeing disc, and D the telescope diameter. Experience of the average seeing conditions at the 1.5-m telescope ($\Delta\theta_s \simeq 2$ arcsec) suggests (see Table 1) that the standard filters adequately meet this requirement apart from the J filter which is about twice the optimum width. Atmospheric dispersion will also restrict the optical bandwidths and Table 1 includes an estimate of the angular spread in the image using the standard filters for a zenith angle of 60°. The corresponding loss in speckle visibility is small for all observations made within two air masses.

The star images produced by the 1.5-m telescope were observed on many occasions to be less than 2 arcsec in diameter although the telescope has a thin primary mirror. With the mounting of the primary well adjusted, the aberrations were reduced to less than 2 arcsec, and fortunately for our application they were mainly astigmatic. The appropriate line image was chosen, reducing the one-dimensional aberration to less than the average seeing. The system was accurately focused on a bright star by selecting a grating with a spatial frequency matched to the seeing disc size and maximizing the modulated signal.

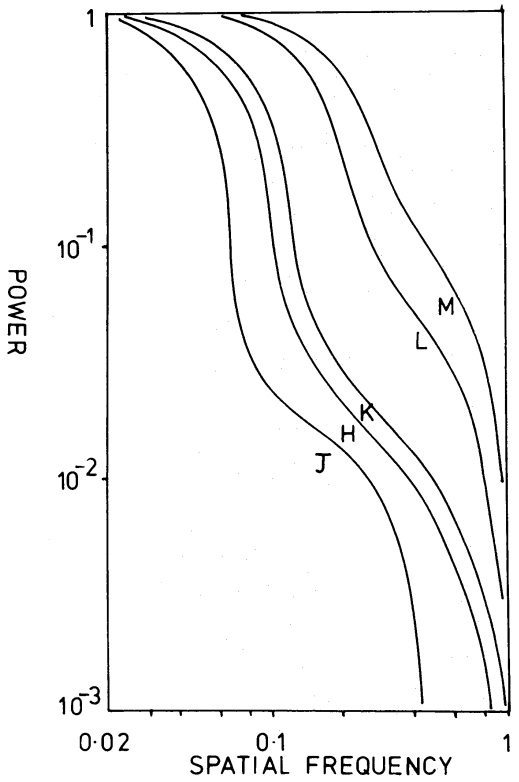

Figure 5. Spatial frequency power spectra of the point source μ UMa at five infrared wavelengths. Spatial frequency normalized to 1 at $\sigma = D/\lambda$.

Fig. 5 shows spatial frequency power spectra of a bright star (point source) at five infrared wavelengths, all taken within 1 hr. They clearly show the profiles to be composed of two components, as suggested by equation (3), and that the speckle transfer function contains information corresponding to the theoretical resolving power of the telescope except in the *J* band. The diffraction-limited components are slightly lower than those predicted theoretically by Korff [16] consistent with the findings of Karo & Schneiderman [17] at visible wavelengths. The steep fall-off at *J* we attribute to the use of a *J* filter which is twice the required bandwidth.

From equation (2) it is clear that in order to determine an object's power transform, the normalized power spectrum of the image intensity must be divided by the normalized power spectrum of a nearby point source. The feasibility of this method must ultimately depend on the stability of the atmospheric fluctuations during the measurement of the source and more importantly over the period including the calibration. Stars within 10° of the source were selected and frequent comparisons were made.

As a test the mean was taken of the normalized power spectra of four calibration stars. Each power spectrum was then divided by this mean so that the spread in these points around unity represents change in the atmospheric transfer function over a typical observation period. The results of these tests are represented by the error bars of Fig. 6.

Also shown in Fig. 6 is a set of data, divided by the appropriate point spread transfer function, for the extended source IRC + 10216 at 2.2 μm. Toombs *et al.* [18] have measured this source using the lunar occultation technique and have fitted their data to a two-shell model with shells of diameter 0.36 and 2″. Although several geometrics can be made to fit the data of Fig. 6, we have found the best fit to be a single Gaussian profile of equivalent width 0.35″.

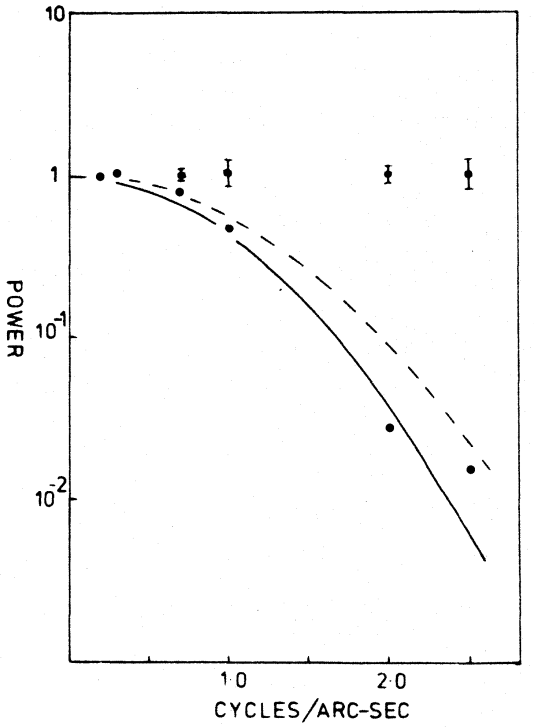

Figure 6. Theoretically predicted power spectra for a source extended to diffraction limit at 2.2 μm (– – –), a source extended to 0.35″ (——), compared with experimental points for IRC + 10216 at 2.2 μm. Error bars represent typical change in normalized MTF over period of observation, determined by ratioing the power spectra of four calibration stars.

Infrared seeing parameters

It has been suggested by Fried [19] that for the near field case ($D \gg (\lambda L)^{1/2}$ where D is the telescope diameter and L is the propagation length through the turbulent medium) the short exposure transfer function of the atmosphere/telescope system can be represented by

$$\langle T(\sigma)\rangle_{SE} = T_0(\sigma) \exp\left[-3.44\left(\frac{\sigma\lambda}{r_0}\right)^{5/3} \times \left(1-\left(\frac{\lambda\sigma}{D}\right)^{1/3}\right)\right] \quad (8)$$

where σ = spatial frequency in the image plane (cycle/rad), $T_0(\sigma)$ = transfer function of the telescope and r_0 is the coherence scale of the wavefront which was defined by Fried as:

$r_0 = (6.88/A)^{5/3}$

where

$A \propto \lambda^{-2}$

so that $r_0 \propto \lambda^{6/5}$ and hence seeing $\propto \lambda^{-1/5}$.

Values of r_0 were obtained by fitting theoretical predictions from equation (8) to measured transfer functions. Fig. 7 shows a set of such results for the different infrared wavelengths, taken over a 1-hr period. The data can be seen to be in reasonable accord with the $^6/_5$ power law shown. The visual seeing was estimated during the observations to be $\cong 3''$ which would lead us to expect the seeing at 2.2 μm to be $\simeq 2.2''$ (if we accept the $^6/_5$ power law); this would give us a value of r_0 at 2.2 μm $\simeq$ 20 cm. This is in fact in reasonable agreement with, although a little higher than, the measured value.

For measurements of the power spectrum of an image at high spatial frequency (large compared to the reciprocal of the seeing disc diameter) the bandwidth of the resulting detector signal is spread predominantly by changes in the image over a characteristic time t_0. Thus the bandwidth of the signal gives a measure of t_0, the temporal correlation width of the image. Fig. 8 shows values of t_0 obtained in this way (adjusted to remove the effects of limited resolution in the power spectrum and limited chop amplitude of the image), for the different infrared wavelengths. The line shown is approximately a half power law. It

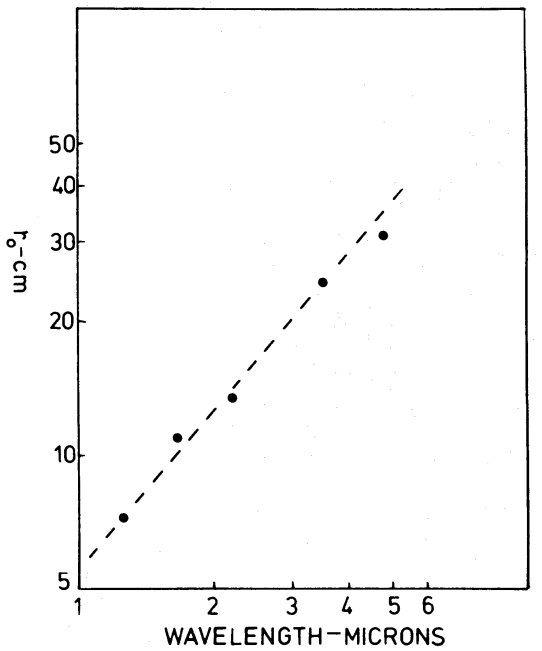

Figure 7. r_0 versus λ; the line shown represents a $^6/_5$ power law.

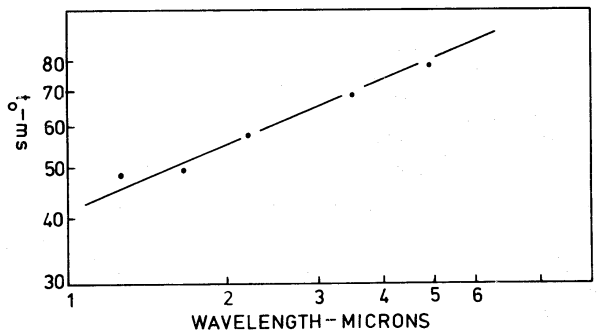

Figure 8. Temporal correlation width t_0 versus λ; the line shown is approximately a half power law.

has been suggested [20, 21] that $t_0 \simeq d/v$ where v is the wind velocity and d is a characteristic scale in the aperture which is of the same order as r_0 but is a function of spatial frequency, so that t_0 should be proportional to $\lambda^{6/5}$. This discrepancy is probably caused by the use of large optical bandwidths.

Speckle limiting magnitudes

In this section we attempt to calculate the limiting magnitude for the 1.5-m telescope and also for larger telescopes, with a discussion of the controlling factors. In the visible the limiting magnitude is ultimately restricted by the shot noise associated with the average number of photons in a speckle [9]. In the infrared the dominant limitation is the shot noise of the infrared background from the atmosphere and telescope, particularly at longer wavelengths.

We proceed by defining the limiting infrared magnitude as that source which can be measured with an angular extension of $\Delta\theta_D = \lambda/D$ with a signal/noise ratio of unity. $\Delta\theta_D$ is

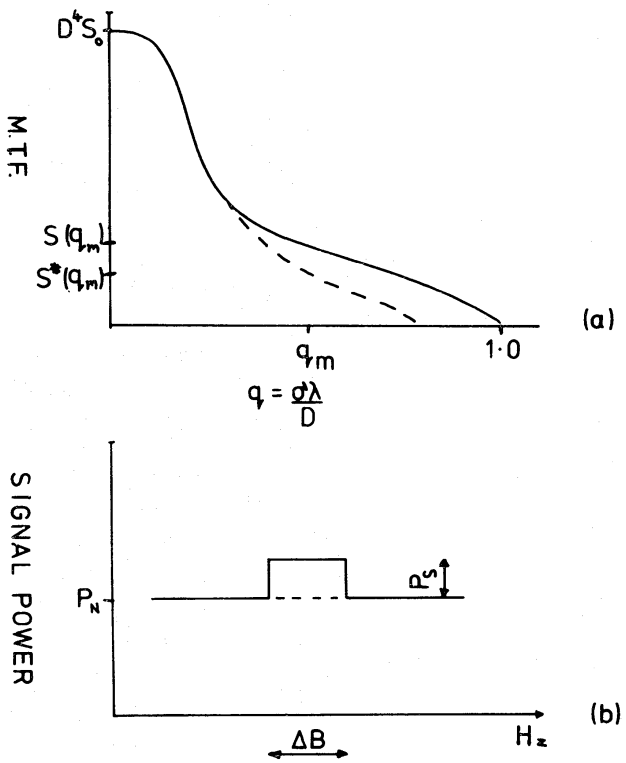

Figure 9. (a) $S(q)$ point spread transfer function. $S^*(q)$ transfer function of source extended to diffraction limit $\Delta\theta_D = \lambda/D$. S_0 is the total squared intensity normalized to a 1-m diameter telescope. (b) Signal power spectrum for measurement of $S^*(q_m)$ when $S^*(q_m) = P_S \Delta B$.

the diffraction-limited resolution and here we consider it to be the 'equivalent width' of the source's angular intensity function. Let $S^*(q)$ be the spatial frequency power spectrum of the extended source image and $S(q)$ the corresponding normalized spectrum of a point source as depicted in Fig. 9(a). $S^*(q)$ and $S(q)$ are sampled at $q = q_m$ and then compared. Here q is the spatial frequency, normalized to 1 at $\sigma = D/\lambda$.

From equation (3) and for $q_m > r_0/D$ we may write

$$S(q_m) \simeq k\beta S_0 D^4 T_D(q_m) \tag{9}$$

where S_0 is the image intensity squared, for a 1-m diameter telescope, corresponding to the speckle limiting magnitude. The factor β is included to take account of the optical filter bandwidth $\Delta\lambda$, selected using the criterion $\Delta\lambda = \lambda^2/D\,\Delta\theta_S$ where $\Delta\theta_S$ is the seeing angle size ($\Delta\theta_S = \lambda/r_0$). If $\Delta\lambda_{phot}$ is the normal photometric bandwidth associated with the width of the infrared atmospheric window, then

$$\beta = (\Delta\lambda/\Delta\lambda_{phot})^2 \quad \text{for} \quad \Delta\lambda < \Delta\lambda_{phot}, \quad \text{otherwise } \beta = 1.$$

It is assumed that when using the technique, the frequency power spectrum of the signal associated with the measurement of $S^*(q)$ takes the form as shown in Fig. 9(b). The signal power $\mathrm{Hz}^{-1}P_S$ is superimposed on the detector noise power $\mathrm{Hz}^{-1}P_N$. As argued previously, it is assumed that the bandwidth ΔB containing the signal power is governed by the temporal coherence in the image, where $\Delta B = 1/t_0$. Generally it can be shown that the signal/noise ratio for a measurement of total noise power P (assuming a 'white' spectrum) taken over a bandwidth ΔB, is given by $(\tau\,\Delta B)^{1/2}$, where τ is the post-detection integration time. It follows that for the measurement of $S^*(q_m)$

$$S^*(q_m) = P_S\,\Delta B \tag{10}$$

with a signal/noise ratio

$$S/N = P_S(\tau\,\Delta B)^{1/2}/[(P_S + P_N)^2 + P_N^2]^{1/2}$$

in the case where $P_S \ll P_N$

$$\frac{S}{N} = \frac{P_S}{P_N}\left(\frac{\tau\,\Delta B}{2}\right)^{1/2}. \tag{11}$$

The above equation takes into account that in order to find $P_S\,\Delta B$ it is necessary to measure the background noise power over a total bandwidth of ΔB taken on either side of the signal passband.

In order to resolve the difference between $S^*(q_m)$ and $S(q_m)$ with a signal/noise ratio of unity, then

$$\frac{P_S}{P_N}\left(\frac{\tau\,\Delta B}{2}\right)^{1/2} = \frac{S^*(q_m)}{S(q_m) - S^*(q_m)}. \tag{12}$$

Assuming the extended source has a Gaussian angular profile with an 'equivalent width' $\Delta\theta_D = \lambda/D$, then

$$S^*(q) = \exp(-2\pi q^2)\,S(q). \tag{13}$$

The noise power $\mathrm{Hz}^{-1}P_N$ from the detector may be expressed as

$$P_N = P_D + \beta^{1/2}D^2P_B \tag{14}$$

where P_D is the intrinsic detector noise measured under low background conditions and the second term represents the shot noise of the infrared background.

It is convenient to express the parameters P_D and P_B in terms of the following photo-

metric limiting magnitudes for a 1-m diameter telescope and using an integration time corresponding to a 1-Hz bandwidth.

$$M_{DL} = 1.25 \log_{10} [S_{00}/P_D]$$
and
$$M_{BL} = 1.25 \log_{10} [S_{00}/P_B] \quad (15)$$

where S_{00} is the zero magnitude intensity squared.

Values of these limiting magnitudes are quoted in Table 2. They were calculated from measurements taken on the 1.5-m telescope of the night-time atmospheric emission for one air mass. The measurements were performed at DC with the speckle sky aperture of 20 arcsec diameter, using α Lyr (0.0 mag all wavelengths) with the quoted fluxes from Johnson [22]. Losses in the detector system were appropriately taken into account. The low-infrared background noise was measured using a 63 K cooled baffle over the detector element.

Table 2. Speckle limiting magnitudes for the infrared filters *J*, *H*, *K*, *L* and *M*.

	J	*H*	*K*	*L*	*M*
M_{BL}	15.4	15.3	14.0	10.0	7.0
M_{DL}	14.0	13.7	13.2	12.3	10.9
M_S^*	11.3	11.8	12.0	9.6	7.1

The resulting photometric limiting magnitude may be similarly defined as

$$M_L = 1.25 \log_{10} [S_{00}/(P_D + P_B)] \quad (16)$$

which can be calculated using values of M_{DL} and M_{BL}. From normal photometric measurements of weak sources on the 1.5-m telescope the directly measured limiting magnitudes generally agreed with the predicted values. It is seen from Table 2 that the detector is background limited at the longer wavelengths for $D > 1$ m and partly so at the shorter wavelengths, particularly for large telescope diameters. Apart from night-time measurements, the daytime atmospheric infrared background was also measured and it is interesting to note that the limiting photometric magnitudes did not change significantly at *L* or *M*, whereas a decrease of 1.5 mag occurred at *K*.

We can define the infrared speckle limiting magnitude as

$$M_S^* = 1.25 \log_{10} [S_{00}/S_0]$$
and it follows from equations (9–16) that

$$M_S^* = 1.25 \log_{10} \left[\frac{[1 - \exp(-2\pi q^2)\, m]\, T_D(q_m)\, r_0^2 \beta (\tau t_0/2)^{1/2}\, D^2}{10^{-0.8 M_{DL}} + \beta^{1/2} D^2 10^{-0.8 M_{BL}}} \right] \quad (17)$$

which for background limited conditions ($P_D \ll \beta^{1/2} D^2 P_B$) is given by

$$M_S^* = M_{BL} + 1.25 \log [0.21 r_0^2 (\beta t_0 \tau)^{1/2}] \quad (18)$$

where $q_m = 0.5$ is adopted, which is the approximate optimum value, although M_S^* is not particularly sensitive to changes in this value. The predicted limiting magnitude in equation (18) depends on the atmospheric parameters r_0 and t_0 and should be approximately independent of telescope diameter. The factor β will be unity at the longer wavelengths where even for large telescopes we find $\Delta\lambda > \Delta\lambda_{phot}$, otherwise β is proportional to $1/D$. The dependence of the temporal coherence time t_0 on the telescope diameter is not clear, although it might be expected to increase with increasing *D*.

The speckle limiting magnitudes have been computed from equation (17), see Table 2, using the measured parameters found on the 1.5-m telescope and the following relations

$$r_0 = \frac{(0.5)^{-1/5}}{\Delta\theta_v} \lambda^{6/5} \times 10^6 \text{m}$$

$$t_0 = 4 \times 10^{-2} \lambda^{1/2} \text{s}$$

where $\Delta\theta_v$ is the seeing angle for the visible in radians and λ is in μm.

The theory will only apply if $r_0 \ll D$, which should be valid for large telescope diameters and short infrared wavelengths, but progressively becomes more approximate for small telescopes at longer wavelengths. The predicted speckle limiting magnitudes are particularly sensitive to changes in the infrared atmospheric background and the visible seeing which will depend on the telescope site.

Conclusions

Using relatively simple infrared equipment on a 1.5-m telescope we have shown that it is possible to retrieve diffraction-limited information at near-infrared wavelengths. In our case we restrict this information to give the equivalent angular size of a source in one dimension. From our limited measurements taken over a total period of about two to three weeks the indications are that good calibration is achievable for about two-thirds of the nights. Under the worst situations of changing seeing etc., more calibrations would have been desirable, particularly done more frequently. The angular resolution obtainable on a 1.5-m telescope (see Table 1) is somewhat limited and the infrared speckle technique should prove more useful when used with larger telescope diameters.

The infrared speckle limiting magnitude is dominated by the shot noise of the infrared background for large telescopes. It is also limited by two fundamental atmospheric parameters, the temporal and spatial coherence, and we predict that the limiting magnitude for diffraction-limited resolution will be approximately independent of telescope diameter D for $D \lesssim 5$ m. The use of a small sky aperture is important so as to reduce the infrared background but its size will be ultimately set by the infrared seeing, which from our limited number of measurements we find to be adequately represented by a $\lambda^{-1/5}$ law.

We have used the conventional criterion for diffraction-limited angular resolution $\Delta\theta_D = \lambda/D$ throughout our discussion; however, for strong sources it is possible to measure smaller values. For example, we estimate that to improve the resolution to $\lambda/2D$, the accompanying loss in S/N ratio is compensated for by a source 1 mag brighter. Further improvements in resolution are only accomplished with far greater losses in S/N ratio and the choice of spatial frequency for sampling the image power spectrum becomes more critical. With the angular resolution available from, say, a 4-m telescope for sources brighter than M_S^* (see Table 2) then the speckle technique should prove useful in the near-infrared, particularly for sources where one might expect to find angular changes with wavelength. The quoted limiting magnitudes M_S^* are based on atmospheric conditions being stable over the observation period, and as is perhaps common with the use of the classical stellar interferometer at infrared wavelengths [23], the calibration using a point source may prove to be the practical limitation. The ideal atmospheric conditions required by the two methods are different, the speckle technique not necessarily requiring good seeing conditions.

Acknowledgments

We acknowledge the cooperation of Professor Francisco Sanchez of the Cabezon Observatory of the University of La Laguna, and thank Mercedes Prieto Muñoz for much observational assistance.

One of us (RW) acknowledges receipt of an SRC studentship.

References

[1] Labeyrie, A., 1970. *Astr. Astrophys.*, **6**, 85.
[2] Gezari, D. Y., Labeyrie, A. & Stanchnik, R. V., 1972. *Astrophys. J.*, **173**, L1.
[3] Blazit, A., Bonneau, D., Koechlin, L. & Labeyrie, A., 1977. *Astrophys. J.*, **214**, L79.
[4] Lynds, C. R., Worden, S. P. & Harvey, J. W., 1976. *Astrophys. J.*, **207**, 174.
[5] Beddoes, D. R., Dainty, J. C., Morgan, B. L. & Scaddan, R. J., 1976. *J. Opt. Soc. Am.*, **66**, 11.
[6] McAlister, H. A., 1977. *Astrophys. J.*, **215**, 159.
[7] Morgan, B. L., Beddoes, D. R., Scaddan, R. J. & Dainty, J. C., 1978. *Mon. Not. R. astr. Soc.*, **183**, 701.
[8] Korff, D., Dryden, G. & Miller, M. G., 1972. *Opt. Commun.*, **5**, 187.
[9] Dainty, J. C., 1974. *Mon. Not. R. astr. Soc.*, **169**, 631.
[10] Dainty, J. C., 1973. *Opt. Comm.*, **7**, 129.
[11] Worden, S. P., Lynds, C. R. & Harvey, J. W., 1976. *J. Opt. Soc. Am.*, **66**, 1243.
[12] Knox, K. T., 1976. *J. Opt. Soc. Am.*, **66**, 1236.
[13] Young, A. T., 1974. *Astrophys. J.*, **189**, 587.
[14] Jorden, P. R., Long, J. F., MacGregor, A. D. & Selby, M. J., 1976. *Astr. Astrophys.*, **49**, 421.
[15] Koorneef, J. & Van Overbeeke, J., 1976. *Astr. Astrophys.*, **48**, 33.
[16] Korff, D., 1973. *J. Opt. Soc. Am.*, **63**, 971.
[17] Karo, D. P. & Schneiderman, A. M., 1976. *J. Opt. Soc. Am.*, **66**, 1252.
[18] Toombs, R. I., Becklin, E. E., Frogel, J. A., Law, S. K., Porter, F. C. & Westphal, J. A., 1972. *Astrophys. J.*, **173**, L71.
[19] Fried, D. L., 1966. *J. Opt. Soc. Am.*, **56**, 1372.
[20] Roddier, C. & Roddier, F., 1975. *J. Opt. Soc. Am.*, **65**, 664.
[21] Karo, D. P. & Schneiderman, A. M., 1978. *J. Opt. Soc. Am.*, **68**, 480.
[22] Johnson, H. L., 1966. *A. Rev. Astr. Astrophys.*, **4**, 193.
[23] McCarthy, D. W. & Low, F. J., 1975. *Astrophys. J.*, **202**, L37.

Appendix: errors in the measurement of spatial frequency power of the image

During any half period of the triangle chop of the image $I(x)$, the signal $S_{\sigma'}(x')$, see equation (6), may be expressed in time as:

$$S_{\sigma'}(t) = i_a(\sigma')\,\Delta\sigma\cos\left[2\pi f_0 t + \phi + \Phi(\sigma')\right] \tag{A1}$$

where f_0 is the modulation frequency given by $f_0 = 4af_c/\lambda'$, and f_c is the sawtooth chop frequency. If $I(x)$ remains stationary in time a periodic signal is produced which has a period $1/f_c$ and thus its power spectrum is a line spectrum with harmonic spacing f_c, peaking at frequencies around f_0. It may be shown that the total power of the signal is given by:

$$P(\sigma') = i_a^2(\sigma')\,\Delta\sigma^2 \sum_{n=0}^{\infty}\left[\left(\frac{\cos\Omega\sin\pi(n+n_c) - \sin\Omega\left[1-\cos\pi(n+n_c)\right]}{2\pi(n+n_c)}\right)\right.$$
$$\left.+\left(\frac{\cos\Omega\sin\pi(n-n_c) - \sin\Omega\left[1-\cos\pi(n-n_c)\right]}{2\pi(n-n_c)}\right)\right]^2 \tag{A2}$$

where n is an integer and corresponds to the order of the harmonic,

$\Omega = \phi + \Phi(\sigma')$

and

$n_c = 4a/\lambda'$.

When $4a/\lambda' \to \infty$, the summation term approaches unity and as $4a/\lambda'$ decreases the deviation from unity increases.

Equation (A2) may be simplified by assuming the phase factor Ω to be completely arbitrary and random over the total integration time used for one spatial frequency filter. This should be a valid assumption when using gratings with $\lambda' \ll$ seeing disc size but not so for the coarser gratings when $\lambda' \gtrsim$ seeing disc size. The summation term is now replaced by:

$$\sum_{n=0}^{\infty} \frac{4n^2[1-(-1)^n \cos n_c\pi]}{\pi^2(n^2-n_c^2)^2} - \frac{2\sin^2 n_c\pi}{\pi(n^2-n_c^2)}. \tag{A3}$$

In practice, to eliminate the DC and higher spatial frequency components contained in any grating (mainly DC and odd harmonics), the detector signals are filtered within a passband which terminates at twice the modulation frequency f_0. Values of the above expression (A3) were calculated over the same restricted frequency range ($n = 1 \ldots 2n_c$) for various values of chop amplitude a. It was found that the fractional change is well represented by the empirical expression:

$$\frac{\Delta P}{P}(\sigma) \simeq \frac{1}{6n_c} \sin[2\pi(n_c - 0.55)]. \tag{A4}$$

Equation (A4) may be used to estimate possible errors resulting from chop amplitude instabilities which in practice are only important with the use of the coarser gratings. Also if the chop amplitude remains constant throughout, then the fractional loss for any one grating is constant. For our most coarse grating (2.5 line/mm, where 1 mm ≡ 10 arcsec) and a peak–peak chop of $2a$ = 1 mm, then a 3 per cent change in the amplitude under the worst situation produces ~3 per cent change in $P(\sigma)$. Even for larger changes in chop amplitude, the maximum possible change in $P(\sigma)$ is restricted to ~6½ per cent. These possible errors may be considered tolerable but the use of coarser gratings would require an increase in chop amplitude with an accompanying increase in the size of the sky aperture $A(x)$. It should be noted that the errors associated with the coarser gratings ($\lambda' >$ seeing disc size) should be computed using equation (A2) which gives larger values than equation (A4).

In practice we find a line power spectrum is evident for gratings with $\lambda' \simeq$ seeing disc size (see Fig. 4) but disappears with the finer gratings to form a continuous band centred on the modulation frequency f_0. The bandwidth ΔB for the latter case is controlled by the temporal changes in the image if the chop period $1/f_c \gtrsim t_0$, where $t_0 \simeq 1/\Delta B$.